3 Instrumentation

3.1 Wind Measurement System

The center piece of the N3R instrumentation package is the "best" aircraft turbulence (BAT) probe (Fig. 2). This device was designed, tested, and built as a result of a collaboration between ARL and Airborne Research Australia (ARA) (Crawford and Dobosy 1992; Hacker and Crawford 1999). The housing consists of a 15-cm diameter carbon-fiber hemisphere mounted on a tapered carbon-fiber cone. The housing and cone are mounted on a roughly 2-m long cylinder protruding forward from the nose of the aircraft. The housing contains four solid-state pressure sensors used to measure differential (three) and static (one) pressure from nine pressure ports symmetrically distributed on the hemisphere. The nominal accuracy of these sensors is ±0.05 mb with a response of about 1 KHz. These measurements provide the pressure distribution over the housing from which the relative air velocity may be computed.

Two global positioning systems (GPS) are used on N3R. A dual-frequency Ashtech GPS antenna is mounted on the tapered cone of the BAT probe just aft of the housing. By using differential GPS (DGPS) correction techniques, aircraft position can be measured to within several centimeters relative to a fixed point and ground velocity can be computed to an accuracy of better than 1 cm s^{-1} in the horizontal and 2 cm s^{-1} in the vertical. These data are acquired at a rate of 5 Hz. Three orthogonally-mounted accelerometers contained in the BAT housing are used to augment the GPS position and velocity data to a frequency of 50 Hz.

Aircraft attitude (pitch, roll, and heading) is measured using a Trimble Advanced Navigation System (TANS) vector GPS. The TANS-vector consists of four antennas mounted on the BAT probe housing, on both wings, and the rear of the cockpit. Using carrier-phase techniques, the position of three antennas is measured relative to a master antenna. Manufacturer specified accuracy for aircraft attitude given the geometry of N3R is 0.05°. The TANS-vector GPS acquires attitude data at a maximum rate of 10 Hz. By differencing measurements acquired by accelerometers in the BAT probe housing and by three accelerometers mounted on the aircraft centerline in the back of the fuselage, the frequency range for aircraft pitch and heading are extended up to 50 Hz. Similarly, the frequency can be extended to 50 Hz for aircraft roll by differencing two accelerometers mounted on either wing. This "blending" technique of aircraft position, velocity, and attitude from data acquired by GPS and accelerometers is described by Eckman et al. (1999).

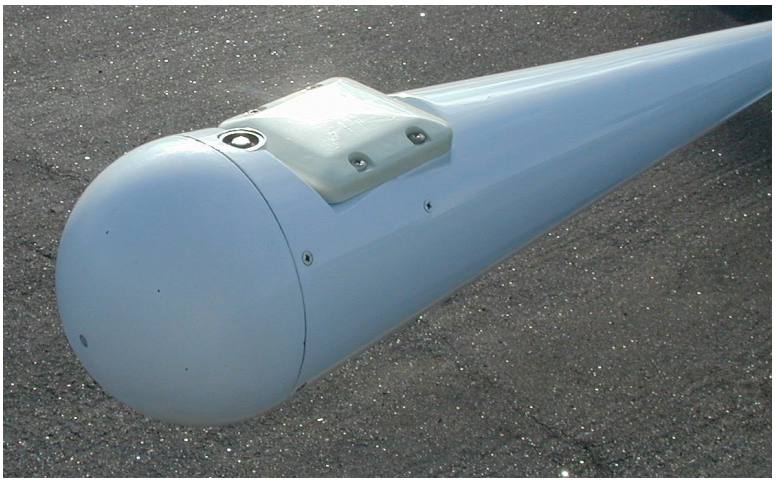

Fig. 2. BAT probe and GPS antenna.

Calibration of the differential pressure sensors is accomplished using a Mensor 4040 digital pressure transducer. The Mensor transducer and the pressure sensors are connected in parallel to a syringe that is used to adjust the pressure applied to both the calibration standard and sensors. The y- and z-axis sensors (lateral and vertical, respectively) are designed to respond to differential pressure of ±15 mb corresponding to an output of ±5 V. The x-axis sensor (longitudinal) ranges from 0 to 28 mb with a corresponding output of ±5 V. Figure 3 shows the linear calibration curves for the Px (longitudinal), Py (lateral), and Pz (vertical) pressure sensors. At least seven independent calibration points (*N*) were acquired for each sensor. A nearly perfect linear correlation *r* exists for all three sensors. The standard error SE, (i.e., the standard deviation about the linear fit) varies between 0.013 and 0.023 mb.

The accelerometers are calibrated by tipping the sensors to known angles and calculating the contribution due to gravity *g* as a function of angle 2 (i.e., $g\sin 2$ or $g\cos 2$). It is possible to produce a calibration curve over the entire range of the device by making measurements over several angles. Figure 4 shows the linear calibration curves for the Ax (longitudinal), Ay (lateral), and Az (vertical) accelerometers located in the BAT probe. At least seven independent calibration points were acquired for each sensor. A nearly perfect linear correlation *r* exists for all three sensors while values of *SE* vary between 0.024 and 0.053 m s^{-2}. The same calibration procedure was performed on the "backseat" accelerometers located along the aircraft centerline in the back of the fuselage (Fig. 5). Once again, values of *r* approach unity. Values of *SE* for all three backseat accelerometers are quite small (~ 0.008 to 0.015 m s^{-2}).

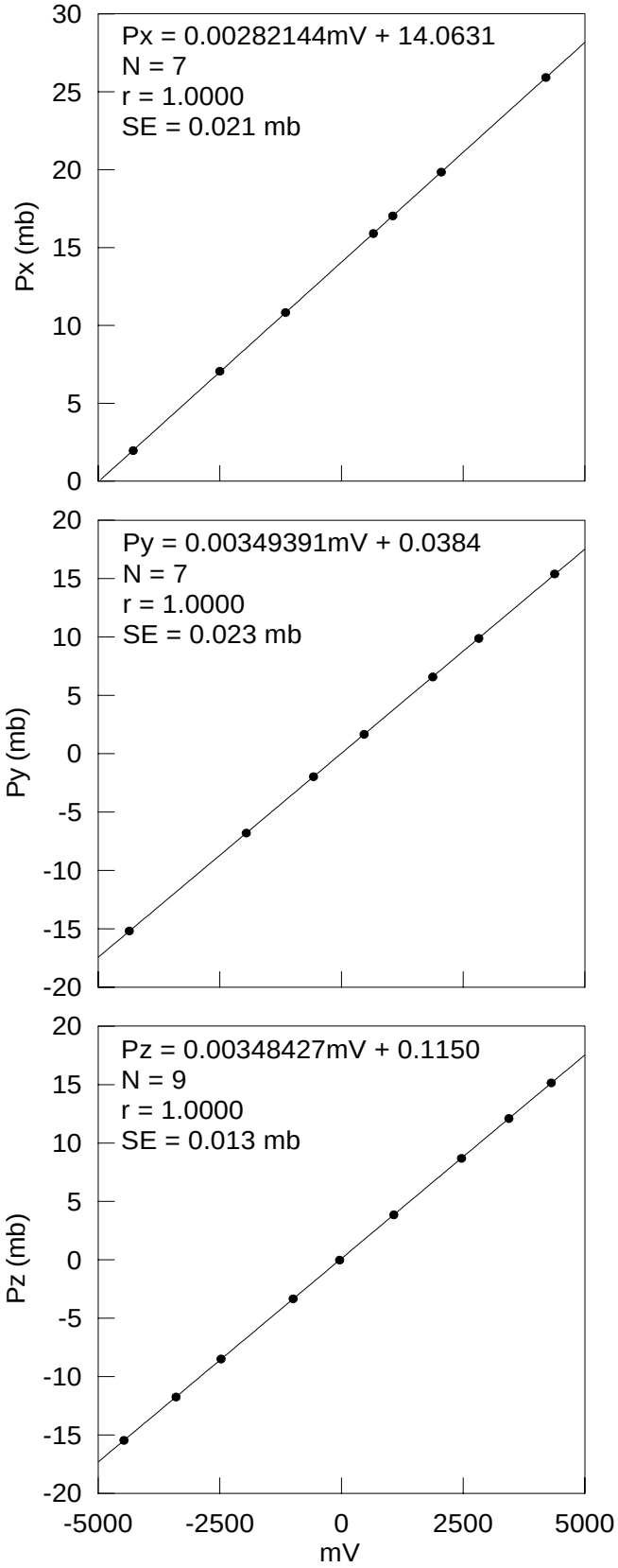

Fig. 3. Calibration curves for BAT probe pressure sensors.

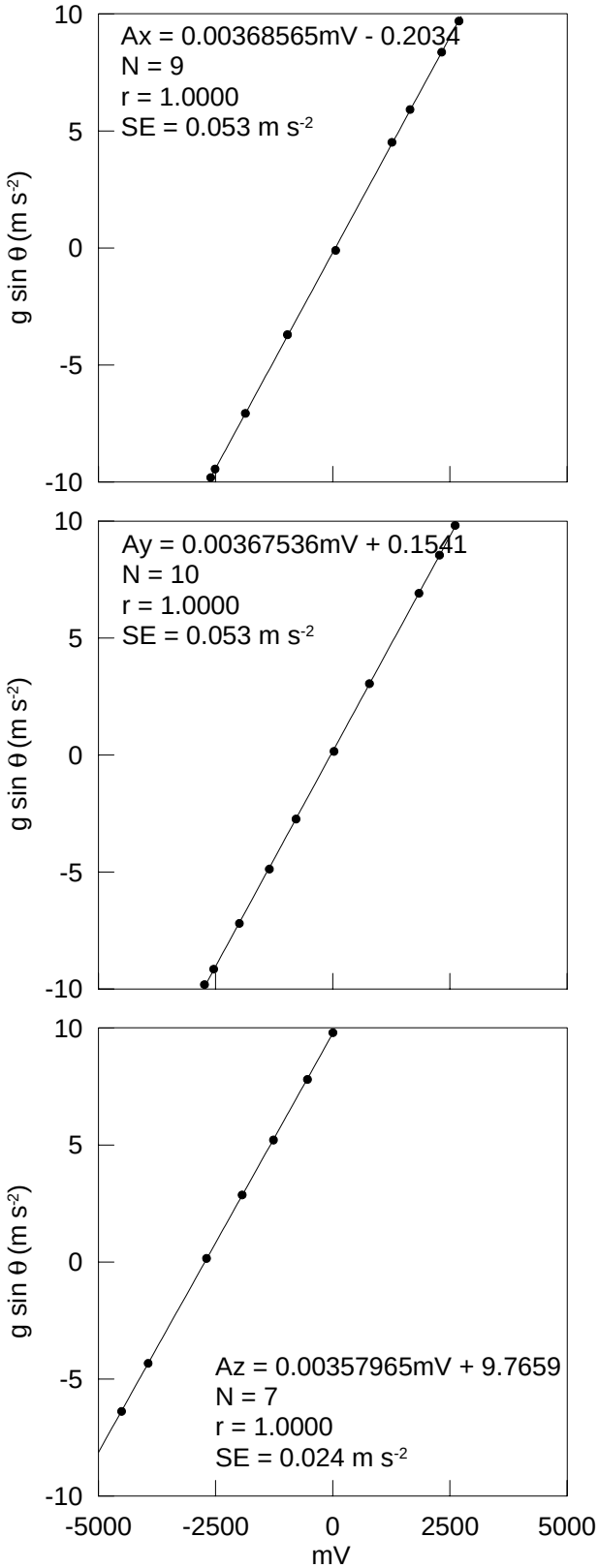

Fig. 4. Calibration curves for BAT probe accelerometers.

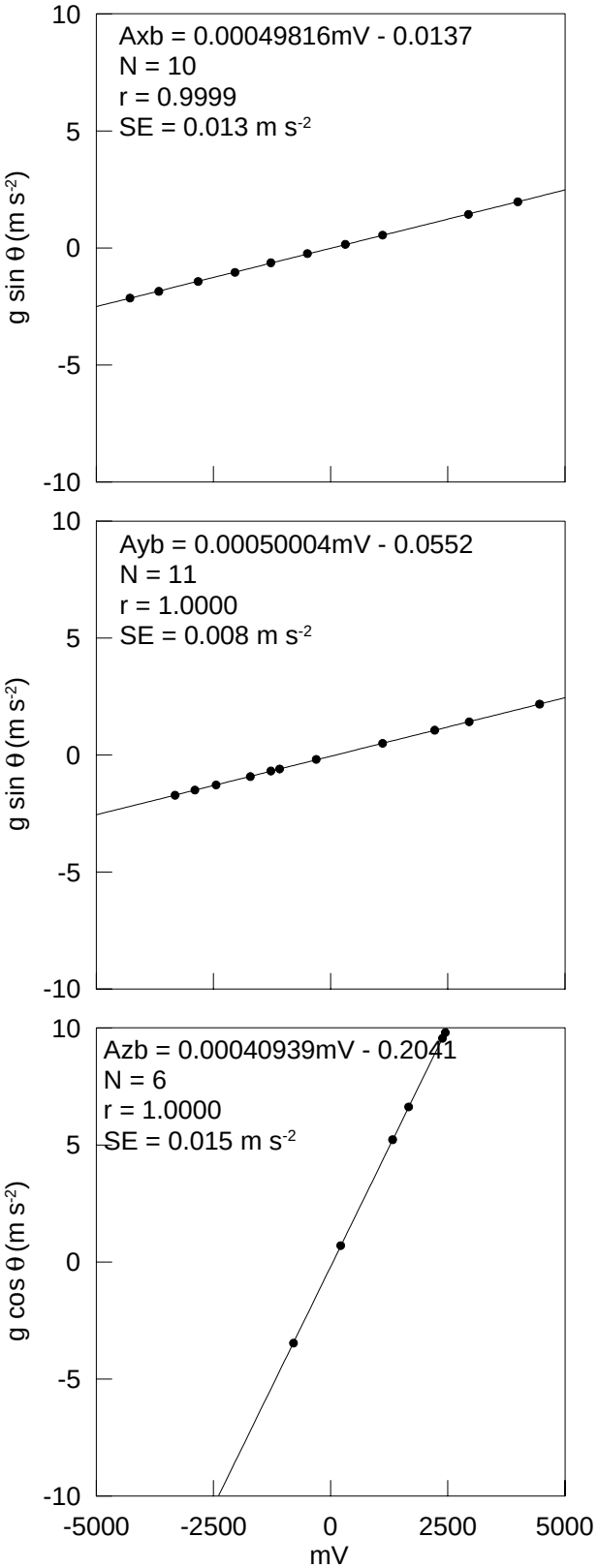

Fig. 5. Calibration curves for backseat accelerometers.

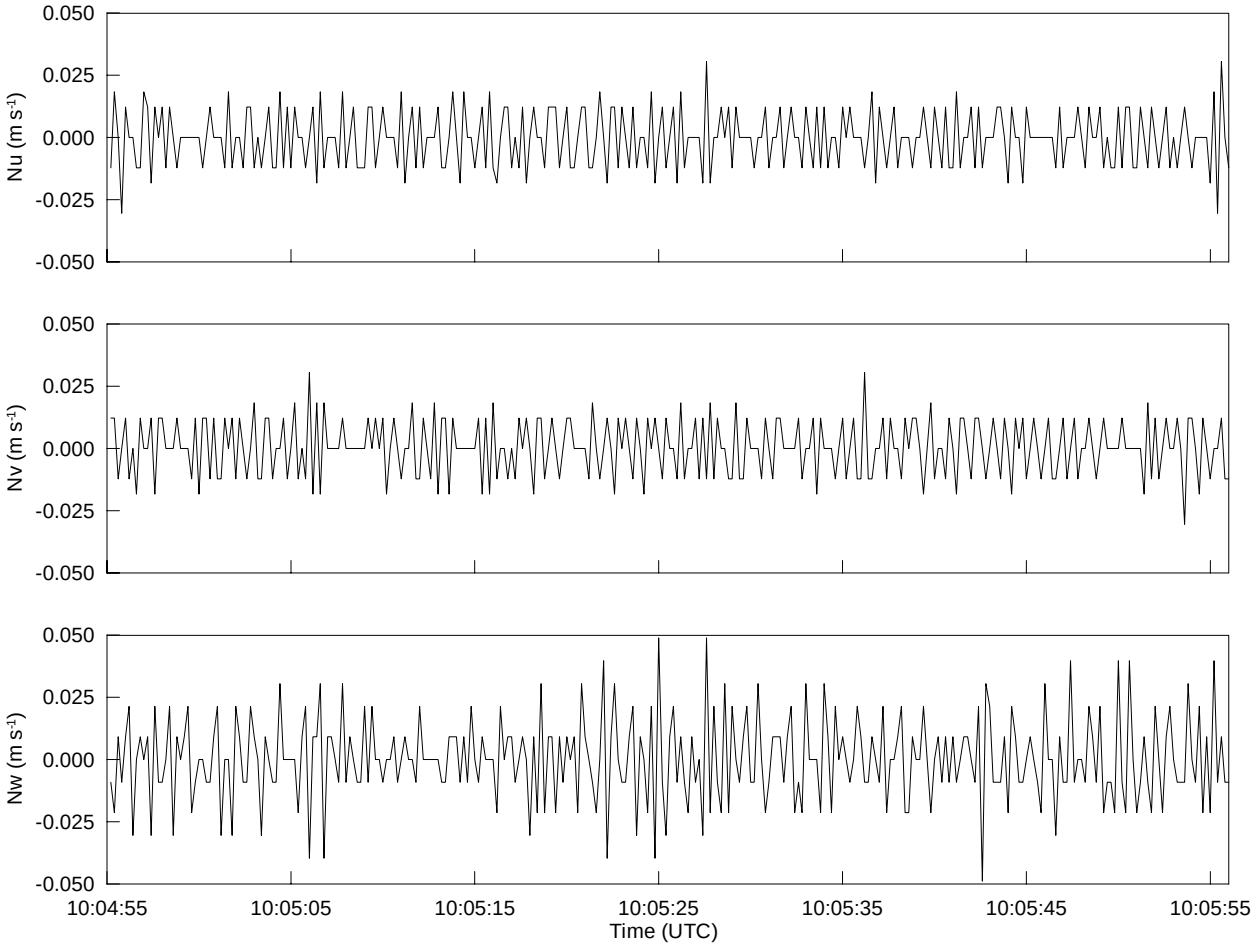

Fig. 6. Demonstration of accuracy of DGPS-derived aircraft velocity. Eastward (Nu), northward (Nv), and vertical (Nw) velocity components are reported for a one-minute period when N3R was stationary on 22 JUL 01.

The Ashtech and TANS-vector GPS are not calibrated per se, but checks are incorporated to ensure the data are within tolerance levels. For example, aircraft velocity data should be zero when N3R is parked on the tarmac. Figure 6 is an example of the DGPS eastward (Nu), northward (Nv), and vertical (Nw) aircraft velocity during a static test. This segment corresponds to a time when N3R was parked on the tarmac for about 60 s on 22 JUL 01. Over the course of the study, data from these static tests show a mean aircraft velocity of zero with a standard deviation of 1 to 2 cm s^{-1}. Spectra indicate the noise in the velocity data appears white (i.e., random). Prior studies have shown a standard deviation of 4 to 5 cm s^{-1} (French et al. 2000). This improvement is due in part to a combination of an upgraded GPS system (from the signal-frequency NovAtel GPS to the dual-frequency Ashtech GPS) and the elimination of selective availability (i.e., artificially inserted noise or variance) in the GPS satellite signals (Showstack 2000).

3.2 Temperature and Humidity Sensors

Three different probes are used to measure air temperature. A slow-response, multi-element

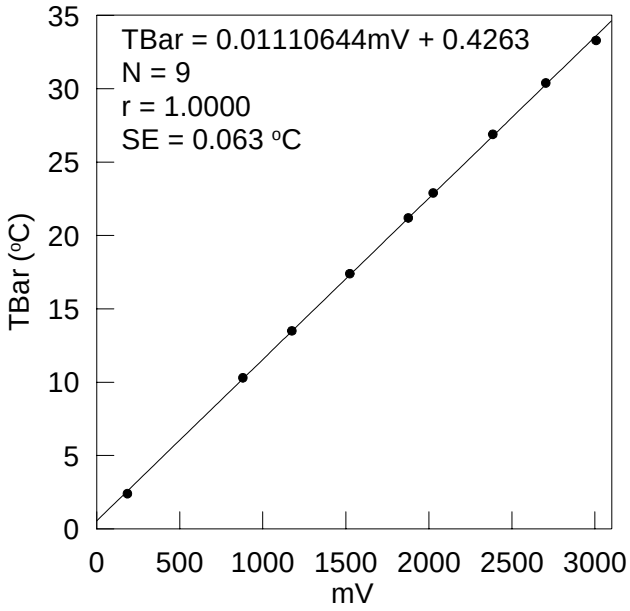

Fig. 7. Calibration curve for slow-response thermistor (TBar).

linear thermistor provides low frequency (1 Hz) temperature measurements. This sensor is mounted within the center-hole, or design stagnation point (DSP) port, on the BAT hemisphere. A second fast-response (~ 20 Hz) 0.13-mm micro-bead thermistor is also mounted inside the DSP port. The recovery factor for micro-bead thermistor is 0.82 (the current housing/element combination has a time constant of ~ 0.07 s). The calculation of the correction factor due to compression is simpler than that of conventional temperature probes because of the location of the sensors within the DSP. The third sensor is the fast ultra-sensitive temperature (FUST) probe (French et al. 2001). This sensor is a Cu-Co 0.025-mm thermocouple and has a response time of better than 20 ms (50 Hz). The probe is mounted on a post below the hemisphere of the BAT probe. The FUST probe is still in the experimental development stage. Results from this new sensor will be documented at a later date.

Humidity is measured with two different sensors. An EG&G 200 chilled mirror sensor provides dew point temperature. This sensor has a relatively long response time (as much as a few seconds). An ARL designed and built fast-response (~ 50 Hz) open-path infrared gas analyzer (IRGA) measures the attenuation of light due to H_2O and CO_2 through a known path (Auble and Meyers 1992**)**.

The slow-response thermistor is calibrated against an accurate mercury-bulb thermometer in a well mixed water bath over a range of temperatures. This method provides a stable calibration. The calibration curve for this thermistor (TBar) is shown in Figure 7. The correlation coefficient is nearly perfect with a standard error of about 0.06 °C.

The fast-response micro-bead thermistor is calibrated in flight against the output from the slow-response thermistor. Figure 8 is a scatter plot of the calibrated temperature acquired by the fast-response thermistor (Tp1) as a function of the slow response thermistor temperature (TBar).

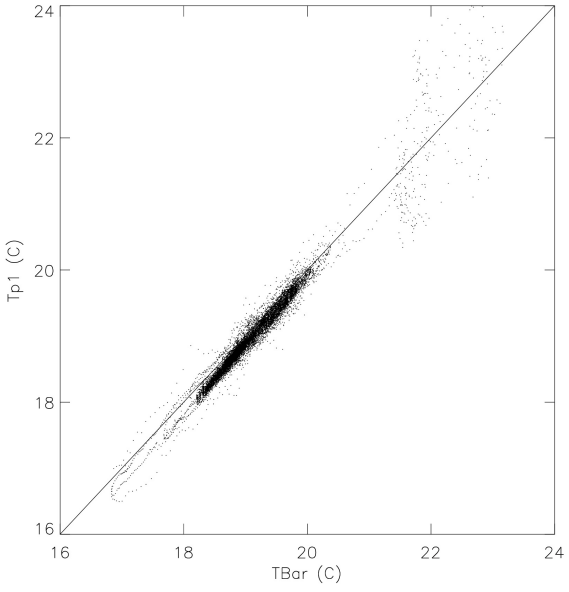

Fig. 8. Scatter plot of temperature acquired by the fast-response thermistor (Tp1) against the slow response thermistor temperature (TBar) acquire by N3R on 21 JUL 01.

In general, temperature data acquired by the micro-bead thermistor is highly correlated with data from the slow-response probe with correlation coefficients usually exceeding 0.9. It should be pointed out that some departures, especially for extreme values, represent real differences in the response time of the two sensors. For example, there are instances where the temperature from the slow-response thermistor changes more slowly than that of the micro-bead thermistor when N3R is flying through strong temperature gradients.

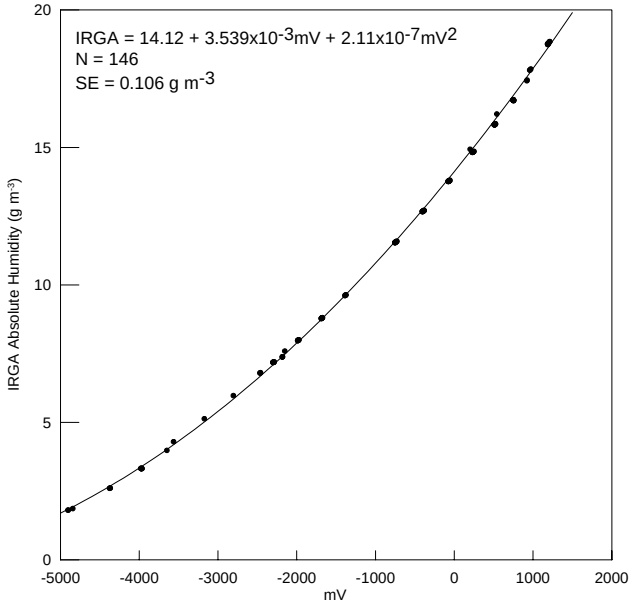

Fig. 9. Calibration curve for IRGA.

The factory calibration was used for the chilled mirror dew point sensor. Data output from this sensor were checked against humidity data acquired by a fan-aspirated psychrometer. The IRGA was calibrated by placing the sensor inside a chamber with known concentrations of water vapor between 2 and 19 g m^{-3}. The calibration curve for the IRGA is a second-order polynomial (Fig. 9). It should be pointed out that values outside this range can be subject to larger errors. For very dry conditions, the IRGA can not acquire reliable data when absolute humidity is less than 1.7 g m^{-3} (corresponding to the minimum sensor output voltage of -5000 mV). Extrapolation of the calibration curve for absolute humidity greater than 19 g m^{-3} can also lead to uncertainty.

3.3 Radiometers

Radiometric sensors mounted on N3R measure both upwelling and downwelling (with respect to the aircraft) radiation. Upward looking and downward looking LI-COR photosynthetically active radiation (PAR) sensors measure the incoming and reflected portion of the visible solar spectrum, respectively. Upward and downward looking Everest Interscience 4000.4GL and 4000.4GXL infrared (IR) radiometer are used to measure sky and sea surface temperature (SST), respectively. The SST radiometer is shown in Figure 10. The upward looking radiometer has a response time of 0.25 s while the downward looking SST sensor has a response time of 0.02 s. The

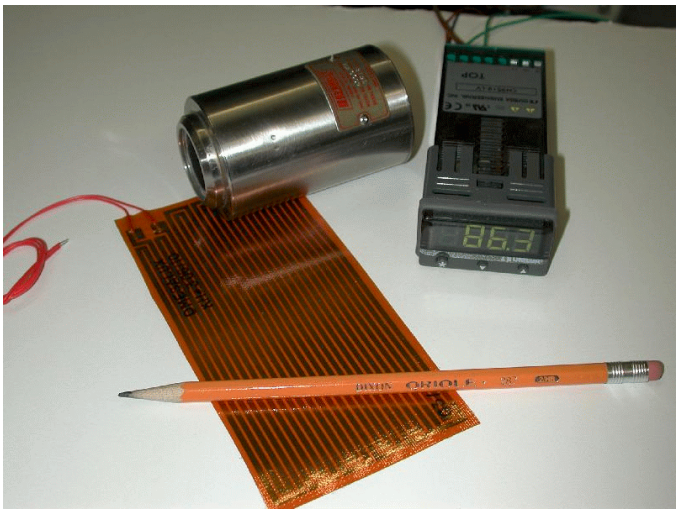

Fig. 10. Everest Interscience 4000.4GXL infrared radiometer with a flexible heater and a temperature controller.

manufacturer specified accuracy for both sensors is ±0.5 ‹C.

The PAR sensors were calibrated against an Eppley Precision Spectral Pyranometer (PSP). These radiometers were placed outdoors under a clear, unobstructed sky for more than eight hours. One minute averages were acquired during this time and were used to determine the calibration curves for the PAR sensors (Fig. 11). Unlike the PSP which is responsive to the entire solar spectrum (0.285 to 2.8 ∶m), the PAR sensors are responsive only to the visible portion of the spectrum (0.4 to 1.1 ∶m). Thus, considerable scatter exists when clouds are present.

The upward looking Everest Interscience 4000.4GL (sky) radiometer was calibrated over a well-mixed water bath over a temperature range of 0 to 40 °C (Fig. 12). The linear regression over this range provides a good fit with an excellent correlation and a standard error of about 0.2 °C. It should be noted that a calibration could not be extended down to -40 °C which is the expected sky temperature for clear conditions.

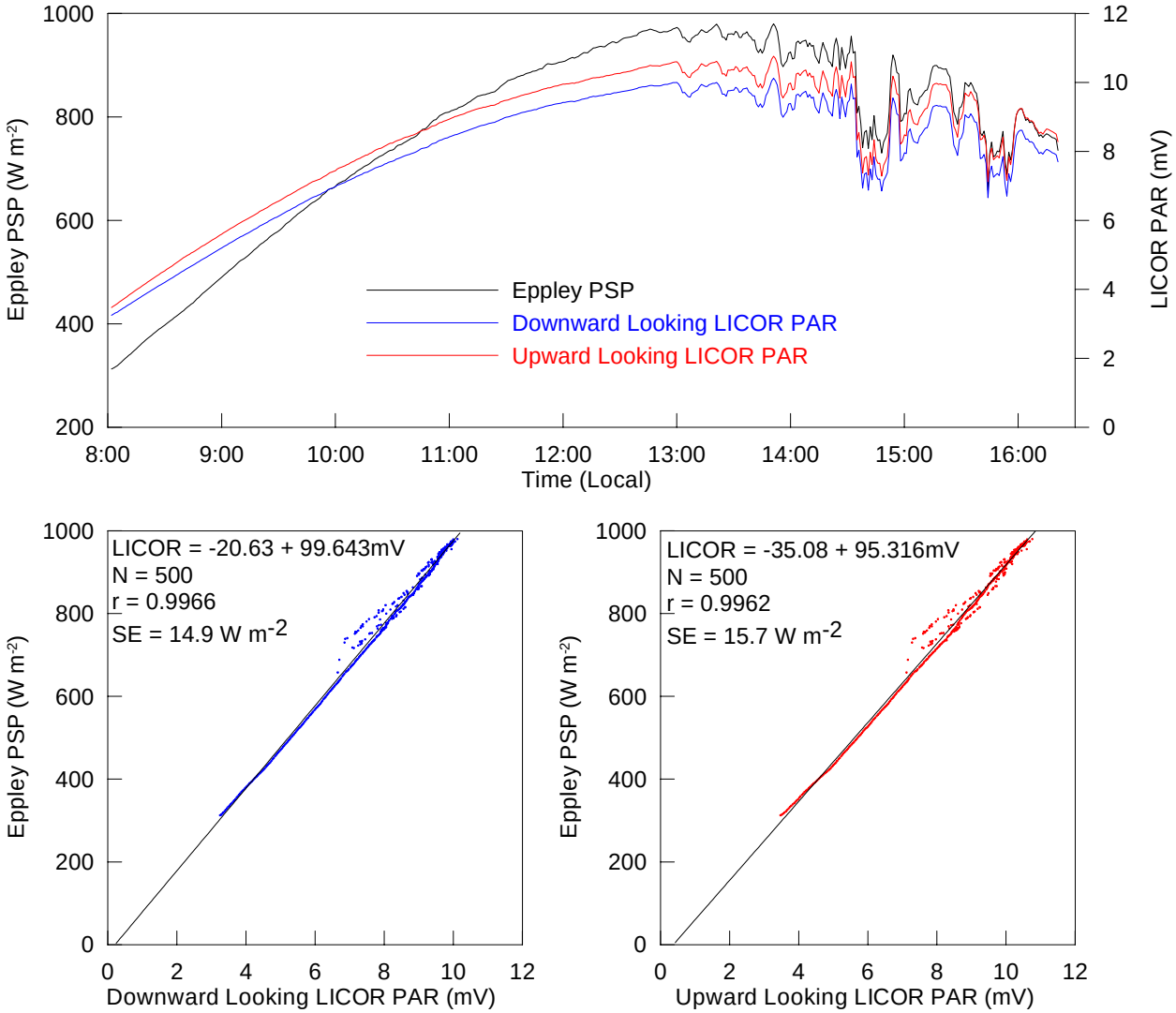

Fig. 11. Calibration curves for PAR sensors.

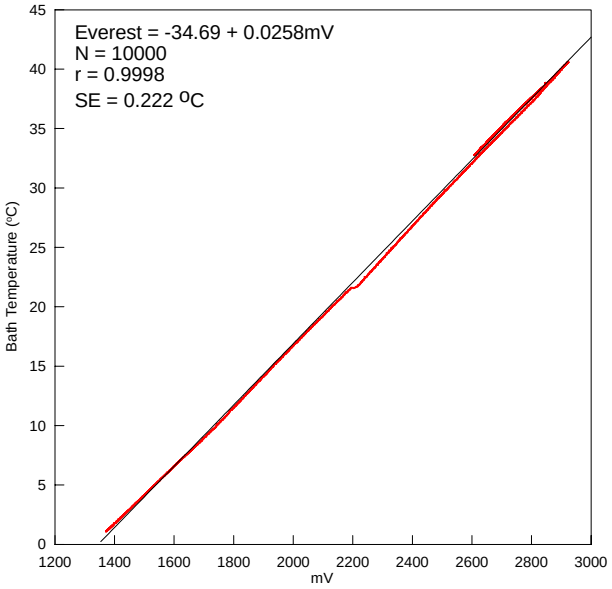

Fig. 12. Calibration curve for Everest Interscience 4000.4GL (sky) radiometer.

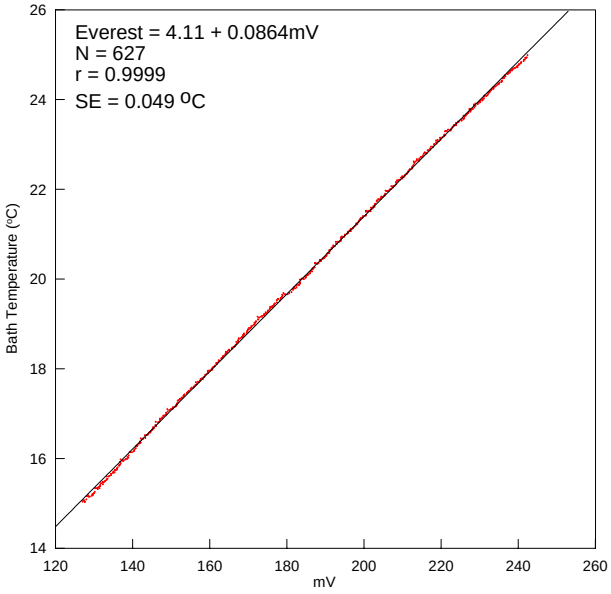

Fig. 13. Calibration curve for Everest Interscience 4000.4GXL (SST) radiometer.

Previous air-sea studies have shown that the SST data are subject to significant errors (> 1 to 2 °C) due to a temperature dependency of the sensor. Laboratory testing showed that SST measurements could be improved to better than 0.2 °C if the body temperature of the radiometer could be kept at a constant temperature. A flexible heater was wrapped around the body of the Everest 4000.4GXL radiometer and encased in a plastic shell with a layer of insulation. A controller is used to maintain a constant sensor body temperature of 30 °C. While the body temperature of the sensor is maintained at a constant value, no corrections are applied for the effects of the intervening atmosphere. The SST radiometer was calibrated over a well mixed water bath over a temperature range of 15 to 25 °C (expected SST off the coast of Martha's Vineyard in the summer). A nearly perfect linear correlation was found for this calibration with a standard error of about 0.05 °C (Fig. 13).

3.4 Ocean Surface Remote Sensors

A laser altimeter array and a nadir-pointing Ka-band scatterometer are used to determine long and short wave characteristics, respectively, of the sea surface. The data obtained from these remote sensors is unique in that it provides wave information from small capillary waves to long swells coupled with wind stress and turbulence measurements acquired by the BAT probe in the atmospheric surface layer. One of the lasers and the scatterometer are carried in an instrument pod suspended beneath the fuselage of N3R (Fig. 14).

Fig. 14. N3R instrument pod.

Fig. 15. Riegl LD90-3100VHS laser altimeter.

An array of three Riegl downward looking laser altimeters is designed to measure the sea surface profile and the one- and two-dimensional slopes of intermediate scale waves on the order of 1 to 10 m (Fig. 15). The laser array consists of three downward looking lasers mounted on the vertices of an equilateral triangle with 1-m separation. Two are mounted under either wing (model LD90-3100VHS) while the third is mounted in the instrument pod (model LD90-3100EHS). These lasers simultaneously measure sea surface height at points about the 1-m diameter circular footprint of the radar scatterometer. The circular footprint of each laser is about 7.5 mm in diameter at an altitude of 15 m. The two lasers mounted in either wing operate with a pulse repetition frequency of 2 KHz while the third laser in the pod operates at a frequency of 12 KHz. The individual pulses are averaged down to a rate of 150 Hz to reduce noise resulting in 13 pulses per scan for the 2-KHz lasers and 80 pulses per scan for the 12-KHz laser. The lasers output distance, normalized amplitude of the returned pulse, and number of valid returns. The focal length of the lasers was set to 15 m providing a nominal accuracy of ±2 mm. The maximum altitude for which the lasers provide useful data is about 50 m. Given the laser measurements and aircraft attitude at any given time, matrix multiplications yield the vector normal to the sea surface plane. Other derived products include significant wave height, dominant wavelength of the wind sea, and the slope variance of the measured two-dimensional probability density function. This last parameter is denoted as the mean square slope (*mss*) of long waves. The *mss* can be considered as the slope variance associated with intermediate scale gravity waves.A fourth Riegl LD90-3100VHS laser was installed in the left wing of N3R at angle of 15° from the vertical. This sensor will serve as a "glint" laser during those instances when the vertically pointing lasers receive few or no returns.

Along-track changes in the integrated roughness of short ocean waves on the order of 2 to 100 cm are determined using a nadir-pointing 36-GHz (8.3 mm) continuous wave scatterometer (Fig. 16). This sensor, developed and built at the National Aeronautics and Space Administration (NASA) by Douglas C. Vandemark, is used to infer the short wave characteristics by relating backscatter intensity to the surface slope variance. The two-antenna remote sensor has a two-way, 3-dB beamwidth of 4.1° which corresponds to a 1.1-m footprint diameter at 15 m. Coincident laser altimeter

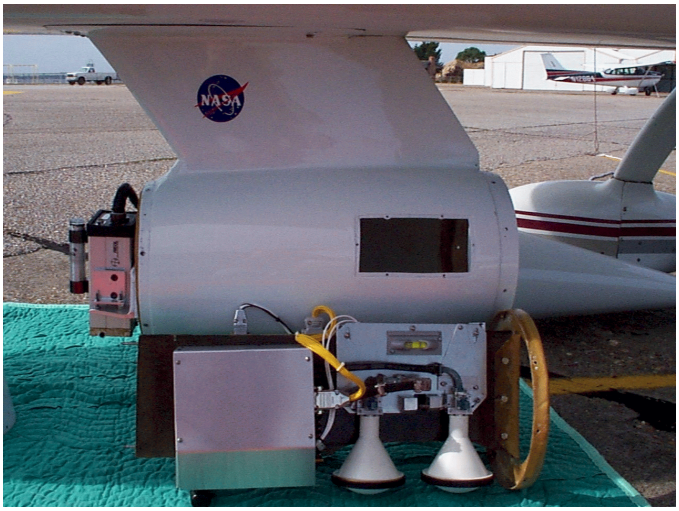

Fig. 16. NASA Ka-band scatterometer.

measurements provide the precise range information for computation of the normalized radar cross section which is used in turn to derive the *mss*. The radar/laser combination leads to high fidelity observations of the long-wave, short-wave hydrodynamic modulation transfer function.

3.5 Other Sensors

An independent suite of remote sensors was also flown by N3R during the CBLAST-Low pilot study. An SST imaging system was developed by Andrew T. Jessup of the University of Washington (UW) and Christopher J. Zappa of the Woods Hole Oceanographic Institution (WHOI). The UW/WHOI system incorporates a Raytheon Galileo IR imager, a Pulnix video camera, a Heitronics KT-15 radiometer, and GPS. The IR imager and video camera were mounted in the rear portion of the instrument pod. The KT-15 radiometer was mounted under the right wing of N3R. These data were acquired and stored on a separate computer and are not included with the N3R data acquisition system.